

Hole-spin qubits in silicon and germanium quantum dots

Andrea Secchi

<https://www.iqubits.eu/>

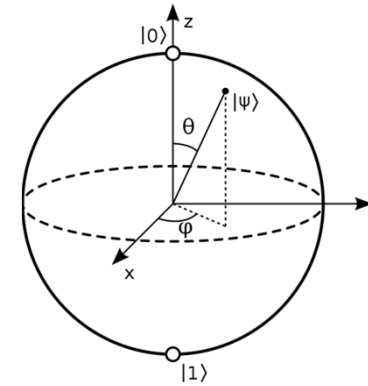


Introduction

Qubit: two-state QM system, basic unit of quantum information

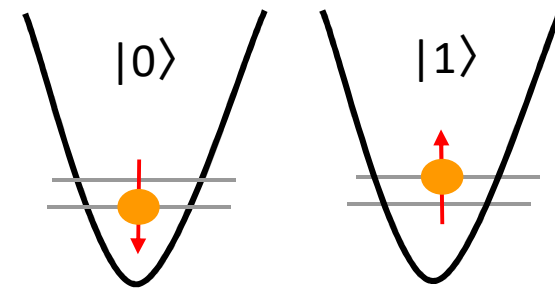
$$|\psi\rangle = \alpha|0\rangle + \beta|1\rangle$$

$$|\alpha|^2 + |\beta|^2 = 1$$



Operations:

- Initialization in a known state;
- Manipulation through quantum logic gates;
- Measurement.



Spin qubits: realized with the «spins» of **localized** charge carriers

Example of two-qubit gate: Loss-Di Vincenzo proposal

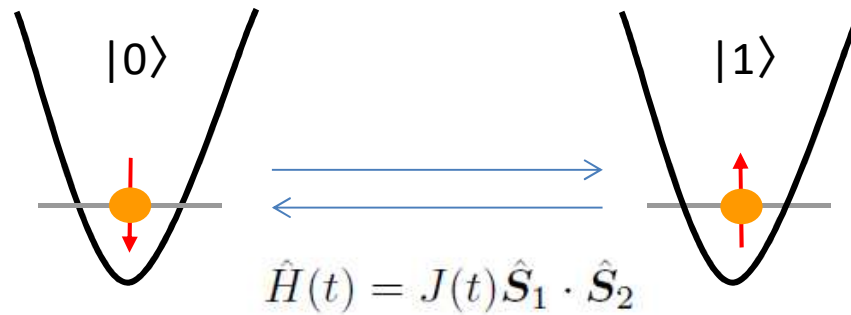
- Double quantum dot (two coupled dots);
- No magnetic field;
- Time-dependent exchange interaction.



Initialization: state 0 in dot 1 and state 1 in dot 2, high barrier between the dots

Example of two-qubit gate: Loss-Di Vincenzo proposal

- Double quantum dot (two coupled dots);
- No magnetic field;
- Time-dependent exchange interaction.



Manipulation: barrier pulsed to low voltage in a time-dependent way

Example of two-qubit gate: Loss-Di Vincenzo proposal

- Double quantum dot (two coupled dots);
- No magnetic field;
- Time-dependent exchange interaction.



After some time: qubit states have been swapped (**SWAP** gate)

Example of two-qubit gate: Loss-Di Vincenzo proposal

- Double quantum dot (two coupled dots);
- No magnetic field;
- Time-dependent exchange interaction.



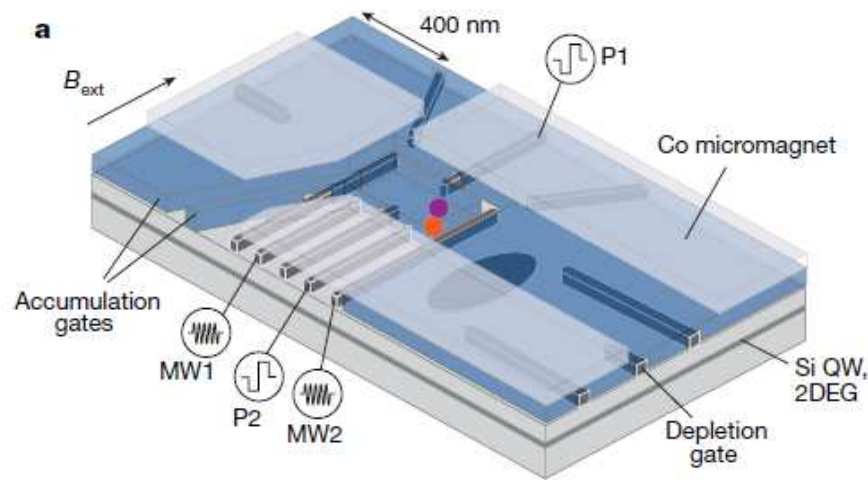
After some time: qubit states have been swapped (**SWAP** gate)

Sqrt(SWAP) + single-qubit gates \rightarrow universal quantum computation

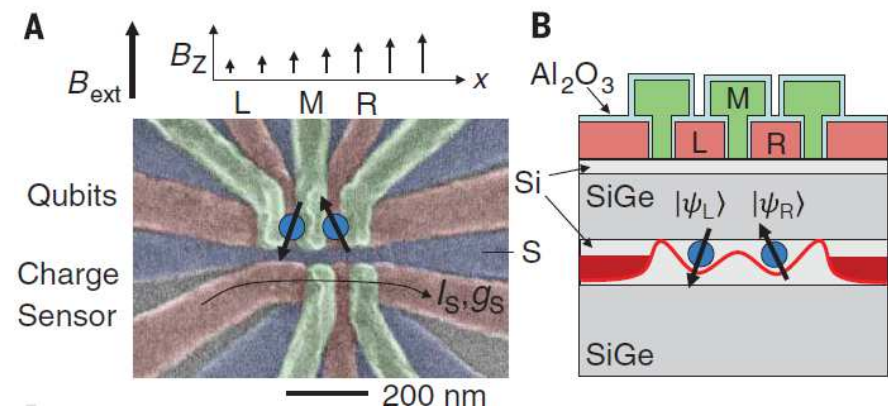
Why silicon and germanium? Why holes?

Why silicon and germanium? Why holes?

- High natural abundance of non-magnetic isotopes ($^{28}\text{Si} + ^{30}\text{Si} > 95\%$ and $^{70}\text{Ge} + ^{72}\text{Ge} + ^{74}\text{Ge} + ^{76}\text{Ge} > 92\%$) + isotopic purification \rightarrow small hyperfine interaction \rightarrow long coherence times

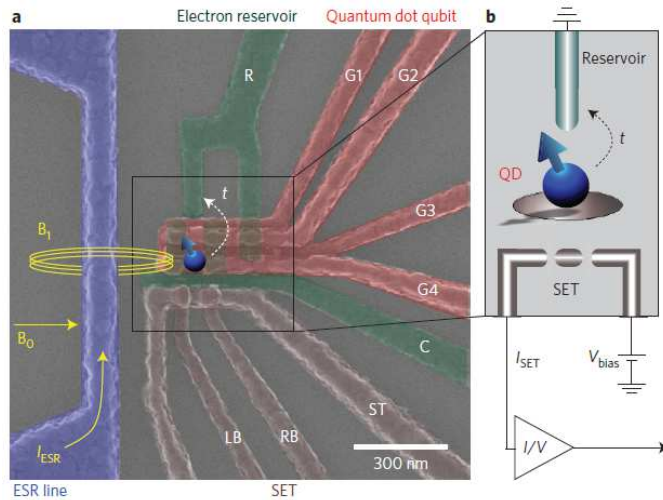


T. F. Watson et al., Nature **555**, 633 (2018)

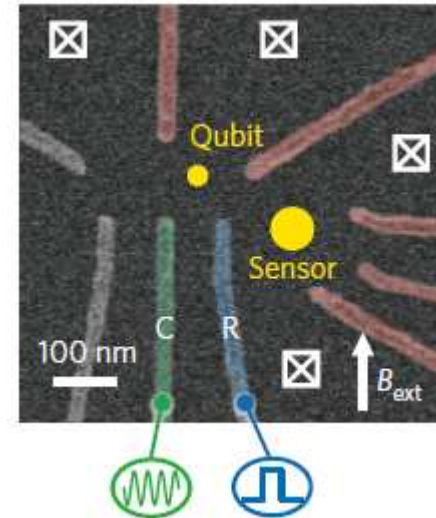


D. M. Zajac et al., Science **359**, 439 (2018)

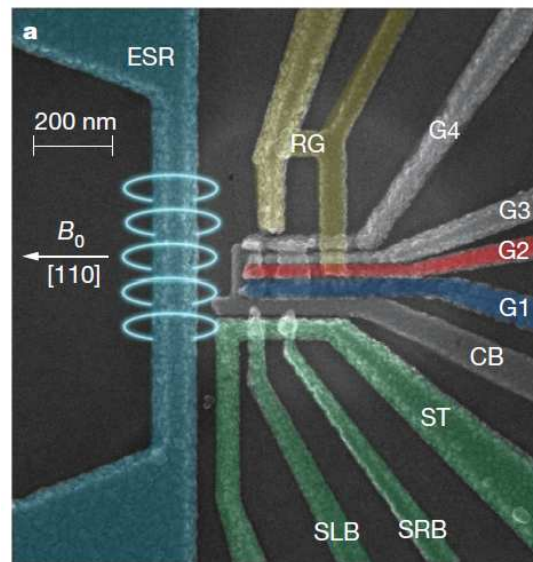
- High degree of control of single and few charge carriers in Si and Ge QDs achieved experimentally during the last decade (gates and readout)



M. Veldhorst et al., Nature Nanotech. **9**, 981 (2014)

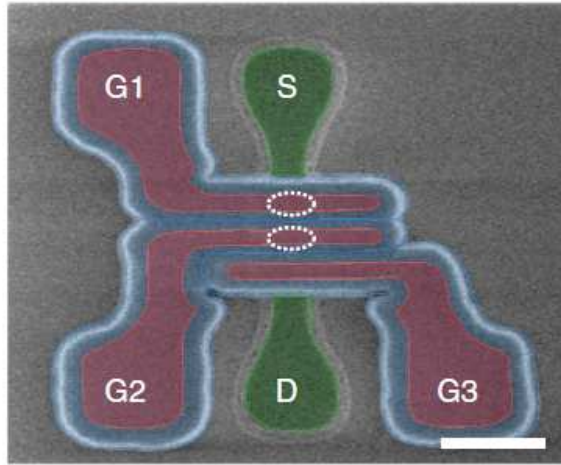


J. Yoneda et al., Nature Nanotech. **13**, 102 (2018)

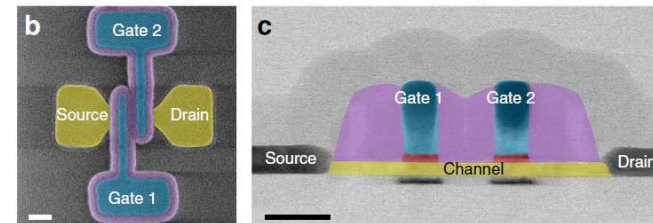
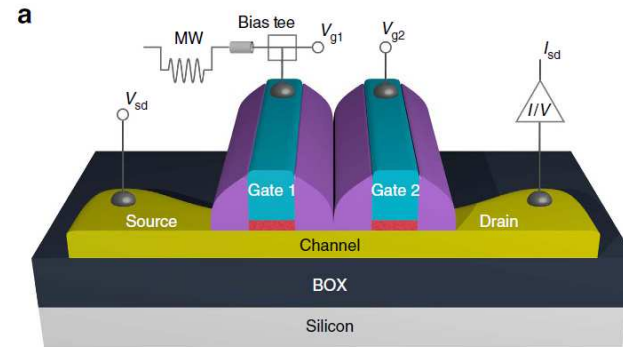


W. Huang et al., Nature **569**, 532 (2019)

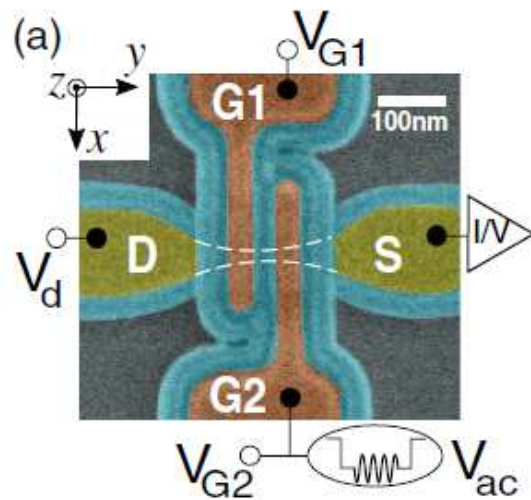
- Key materials for modern electronics → well-established industrial fabrication techniques → integration of qubits and control circuits (CMOS qubits)



M. Urdampilleta et al., Nature Nanotech. **14**, 737 (2019)

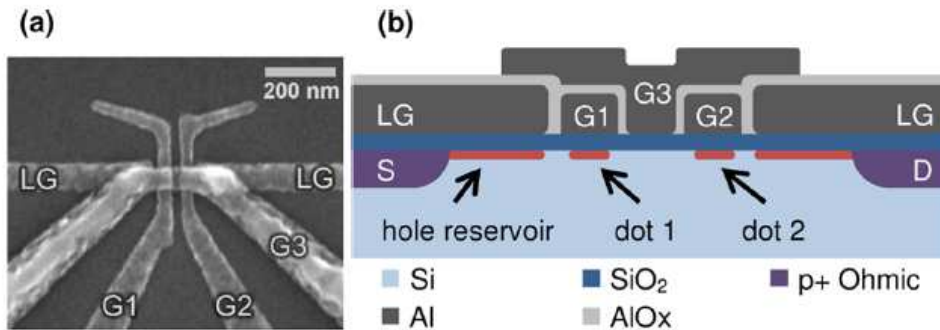


R. Maurand et al., Nature Commun. **7**, 13575 (2016)

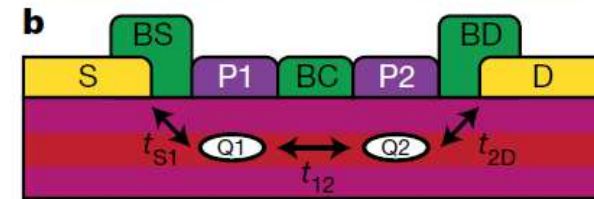
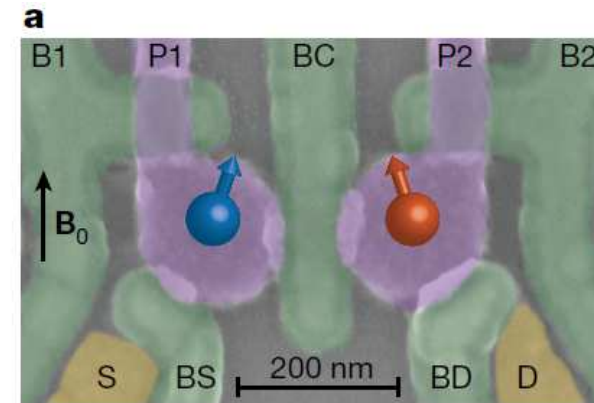


A. Crippa et al., Phys. Rev. Lett. **120**, 137702 (2018)

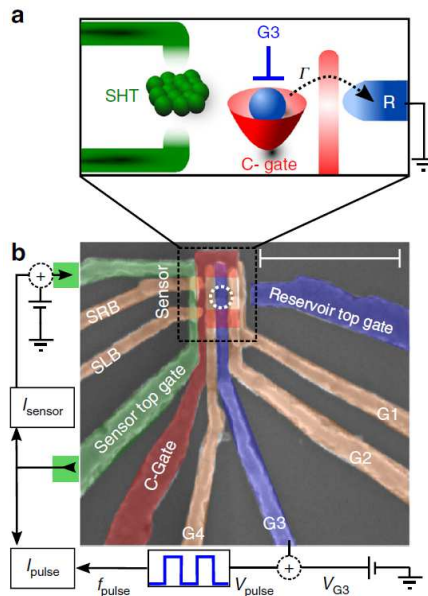
- Valence band made of p orbitals \rightarrow further reduction of hyperfine interaction and larger spin-orbit coupling w. r. to conduction band \rightarrow hole-spin qubits can be manipulated fully *electrically*



R. Li et al., Nano Lett. **15**, 7314 (2015)



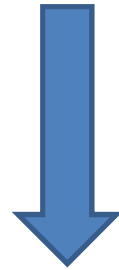
N. W. Hendrickx et al., Nature **577**, 487 (2020)



S. D. Liles et al., Nature Commun. **9**, 3255 (2018)

Main challenge

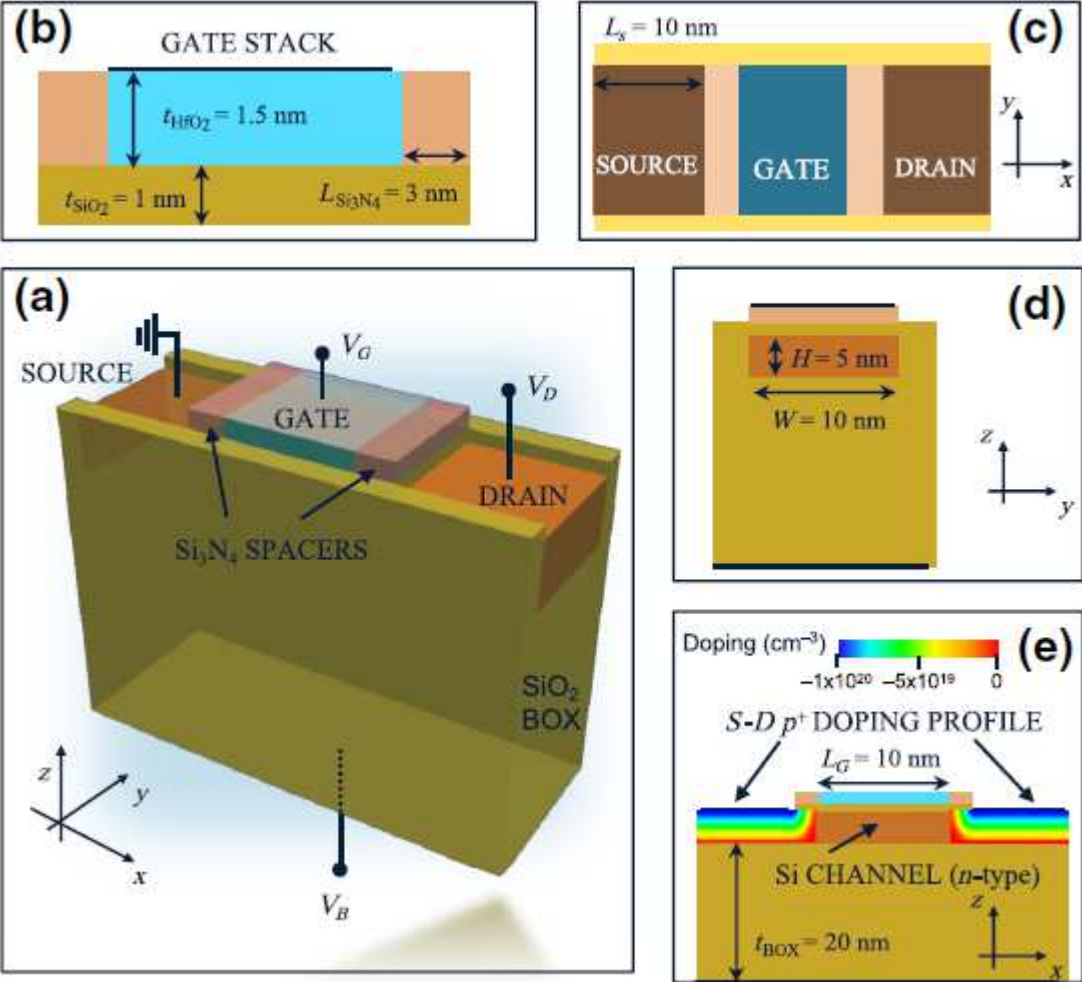
Need to operate the qubit at **millikelvin temperatures** to enhance **coherence times**; need to operate the control electronics at **1-4 K** to allow for a sufficiently fast removal of **dissipated power** → conflicting requirements



Qubit implementation in down-scaled MOSFETs (high quantum confinement → higher excitation energies → possibility of operating the qubit at higher temperatures)

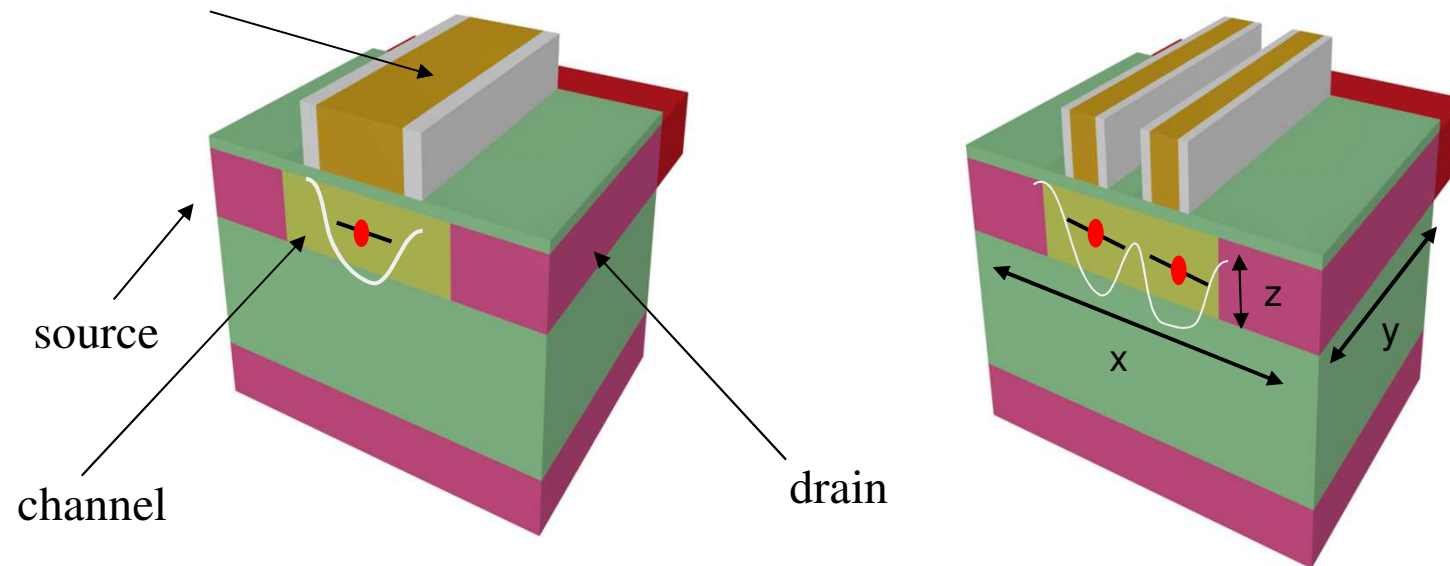
Scaled Si *p*MOSFET (scaled version of GlobalFoundries 22-nm FDSOI process)

Qubit manipulation through voltage pulses applied to the top gate



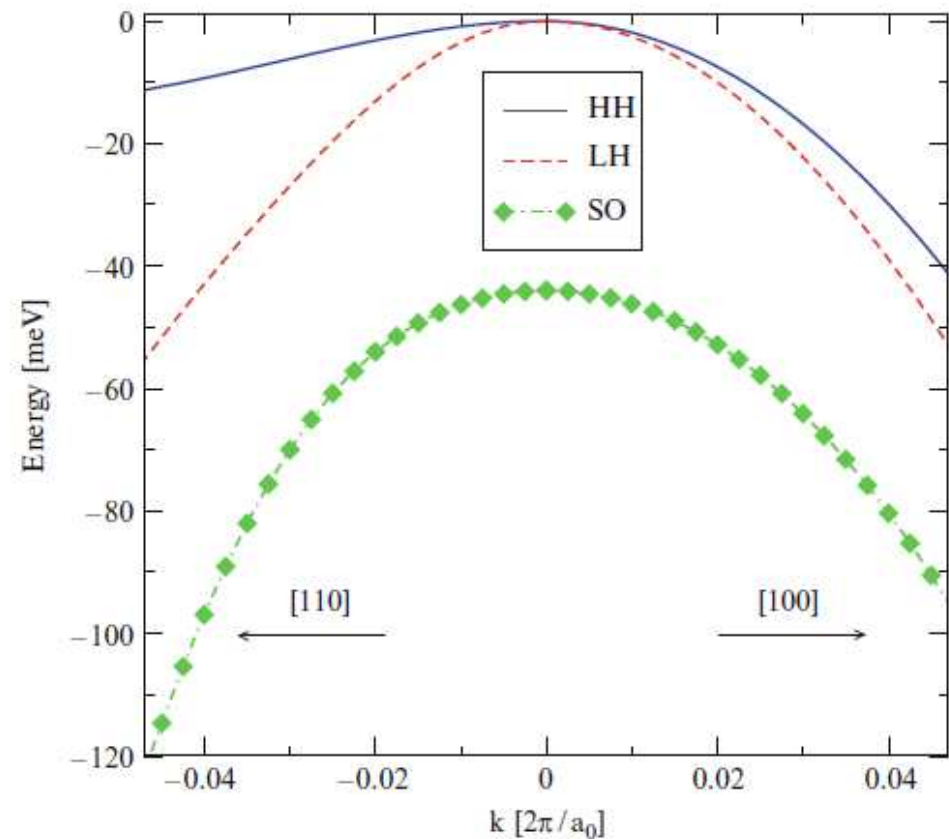
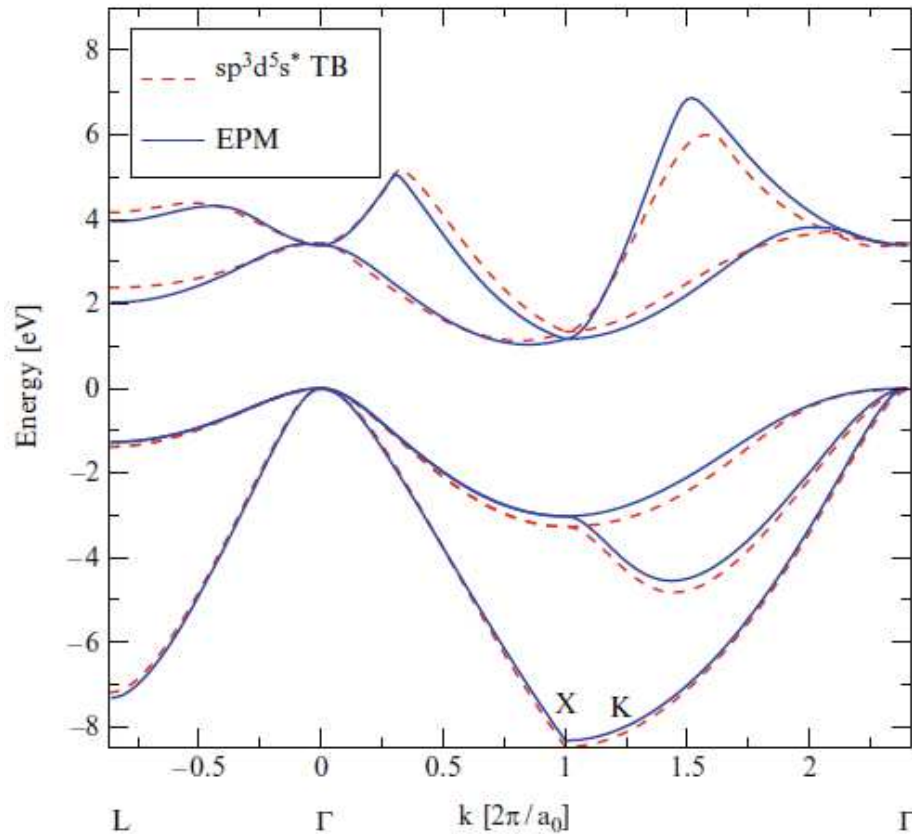
Application of one or more gates to generate single or multiple QD confinement potential inside the Si channel

gate on top of the insulating layer



→ Goal: Investigate the feasibility of one-hole or two-hole qubits in single or double quantum dots

Holes at the Γ point



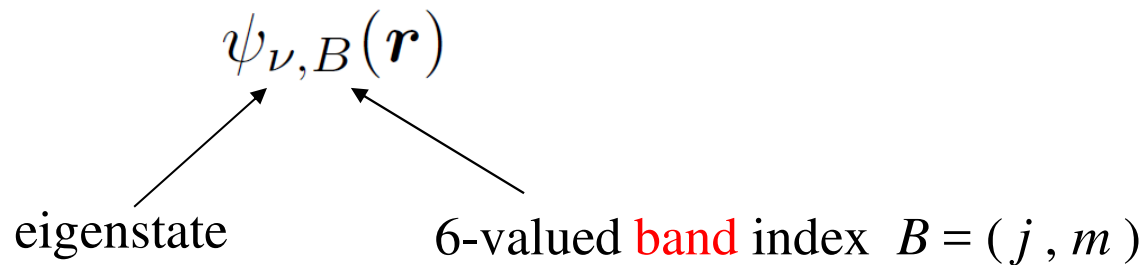
- The unit cell of Si and Ge contains two atoms
- Three p orbitals are relevant for the valence bands at their maximum point (Γ)
- Six Bloch spin-orbital states needed to describe holes at Γ : $j = 3/2$ and $j = 1/2$ multiplets
- $j = 3/2$ and $|m| = 3/2$: heavy holes; $j = 3/2$ and $|m| = 1/2$: light holes; $j = 1/2$: split-off bands

- Including confinement (QD): **envelope function scheme**

basis $\{|\frac{3}{2}, \frac{3}{2}\rangle, |\frac{3}{2}, \frac{1}{2}\rangle, |\frac{3}{2}, -\frac{1}{2}\rangle, |\frac{3}{2}, -\frac{3}{2}\rangle, |\frac{1}{2}, \frac{1}{2}\rangle, |\frac{1}{2}, -\frac{1}{2}\rangle\}$

$$\mathcal{H}_{k,r} = \begin{pmatrix} P_k + Q_k + V_r & -S_k & \tilde{R}_k & 0 & -\frac{1}{\sqrt{2}}S_k & \sqrt{2}\tilde{R}_k \\ -S_k^\dagger & P_k - Q_k + V_r & 0 & \tilde{R}_k & -\sqrt{2}Q_k & \sqrt{\frac{3}{2}}S_k \\ \tilde{R}_k^\dagger & 0 & P_k - Q_k + V_r & S_k & \sqrt{\frac{3}{2}}S_k^\dagger & \sqrt{2}Q_k \\ 0 & \tilde{R}_k^\dagger & S_k^\dagger & P_k + Q_k + V_r & -\sqrt{2}\tilde{R}_k^\dagger & -\frac{1}{\sqrt{2}}S_k^\dagger \\ -\frac{1}{\sqrt{2}}S_k^\dagger & -\sqrt{2}Q_k & \sqrt{\frac{3}{2}}S_k & -\sqrt{2}\tilde{R}_k & P_k + \Delta + V_r & 0 \\ \sqrt{2}\tilde{R}_k^\dagger & \sqrt{\frac{3}{2}}S_k^\dagger & \sqrt{2}Q_k & -\frac{1}{\sqrt{2}}S_k & 0 & P_k + \Delta + V_r \end{pmatrix}$$

- Diagonalization yields the **6-component envelope function**:



Inter- and intra-band interactions

- Two-hole states are obtained via the Configuration-Interaction (CI) method
- Two-body matrix elements of the interaction are required

Textbook expression:

$$V_{\{\nu\}} = \int d\mathbf{r} \int d\mathbf{r}' \psi_{\nu_1}^*(\mathbf{r}) \psi_{\nu_2}^*(\mathbf{r}') V_{\text{Coulomb}}(\mathbf{r} - \mathbf{r}') \psi_{\nu_3}(\mathbf{r}') \psi_{\nu_4}(\mathbf{r})$$

Inter- and intra-band interactions

- Two-hole states are obtained via the Configuration-Interaction (CI) method
- Two-body matrix elements of the interaction are required

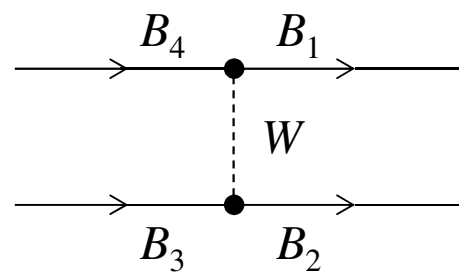
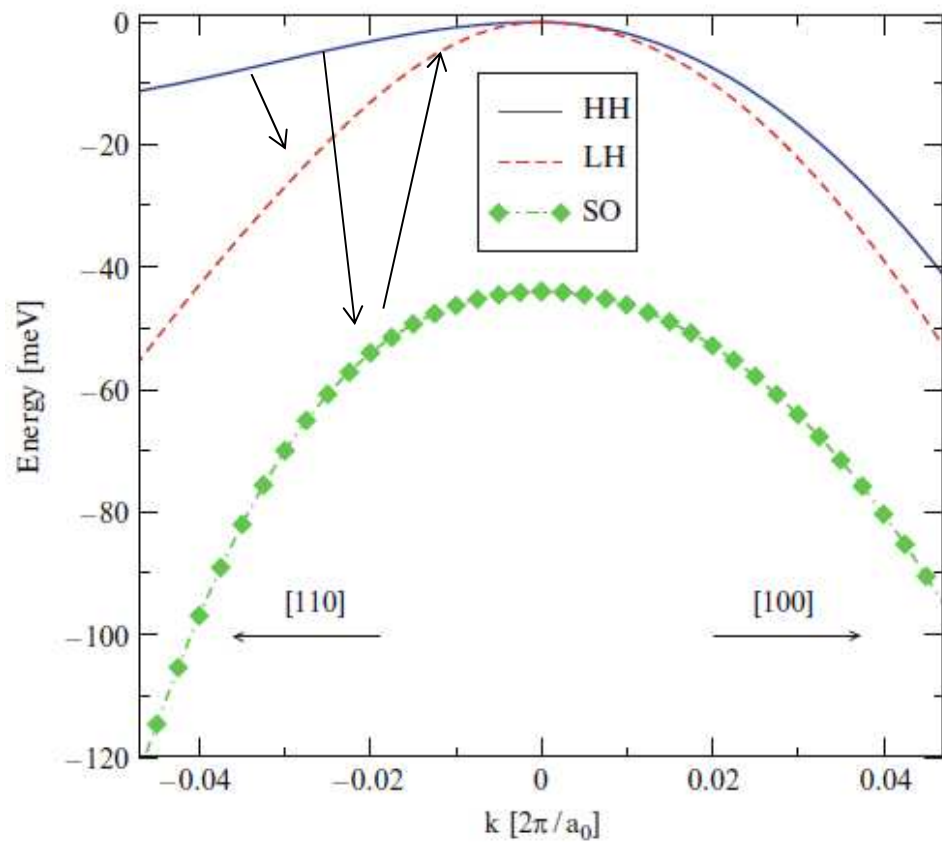
Textbook expression:

$$V_{\{\nu\}} = \int d\mathbf{r} \int d\mathbf{r}' \psi_{\nu_1}^*(\mathbf{r}) \psi_{\nu_2}^*(\mathbf{r}') V_{\text{Coulomb}}(\mathbf{r} - \mathbf{r}') \psi_{\nu_3}(\mathbf{r}') \psi_{\nu_4}(\mathbf{r})$$

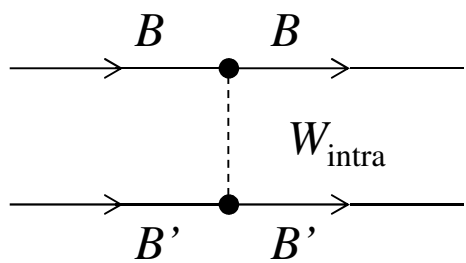
BUT we are dealing with a multi-band system:

$$V_{\{\nu\}} = \sum_{\{B\}} \int d\mathbf{r} \int d\mathbf{r}' \psi_{\nu_1, B_1}^*(\mathbf{r}) \psi_{\nu_2, B_2}^*(\mathbf{r}') W_{B_1, B_2, B_3, B_4}(\mathbf{r} - \mathbf{r}') \psi_{\nu_3, B_3}(\mathbf{r}') \psi_{\nu_4, B_4}(\mathbf{r})$$

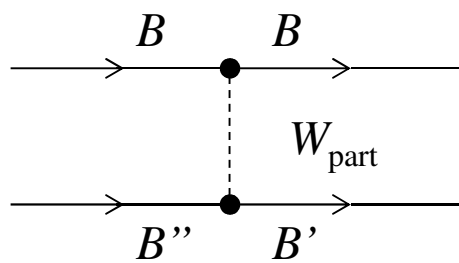
Band-dependent interaction



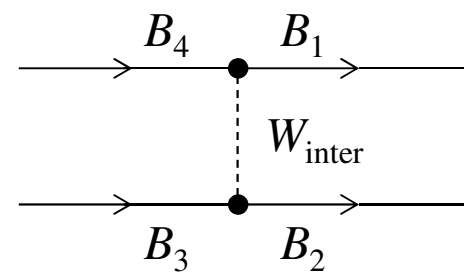
Intraband (36)

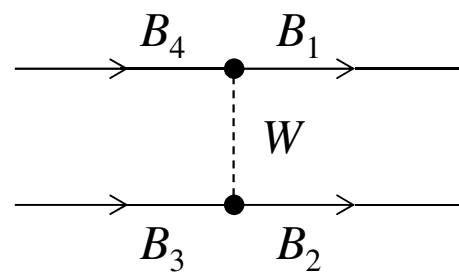
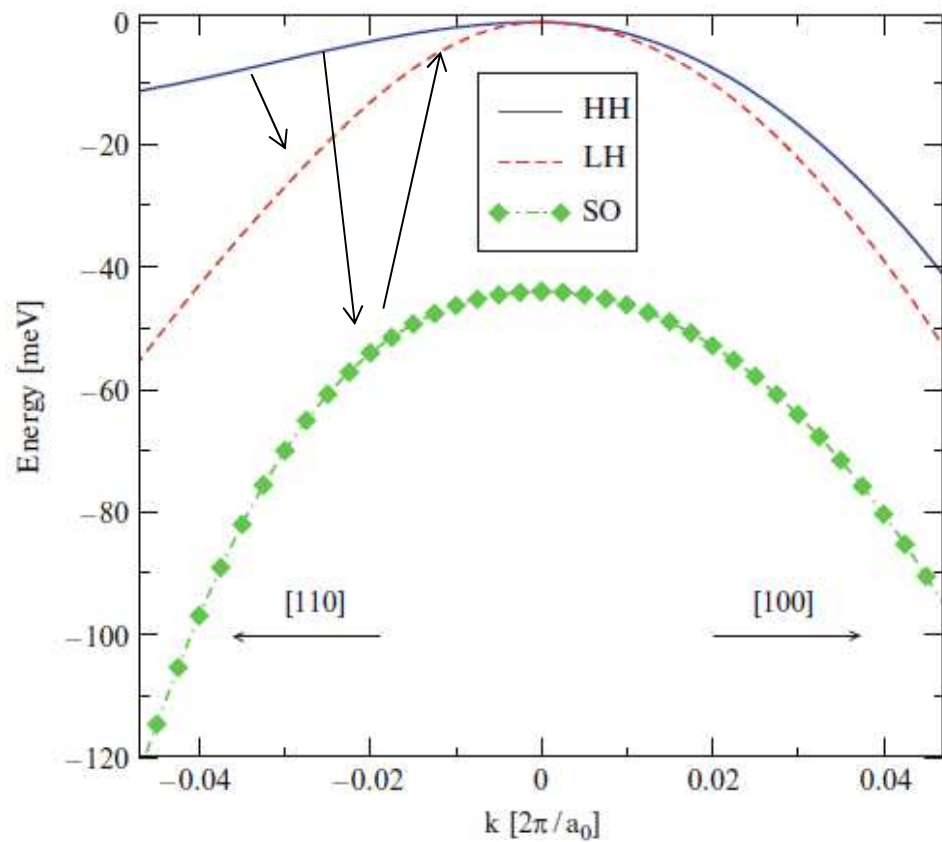


Partially interband (32)



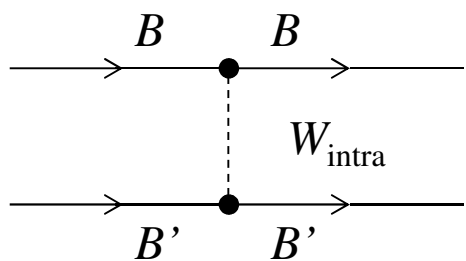
Interband (120)



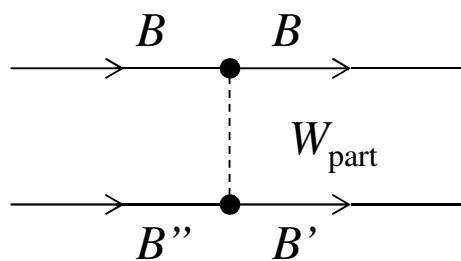


Short-ranged
Relevant for downscaled devices

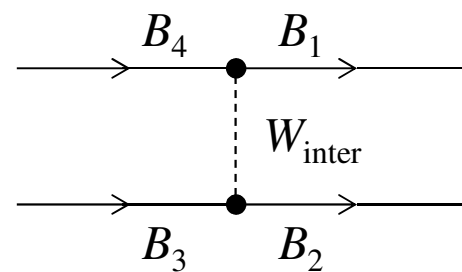
Intraband (36)



Partially interband (32)



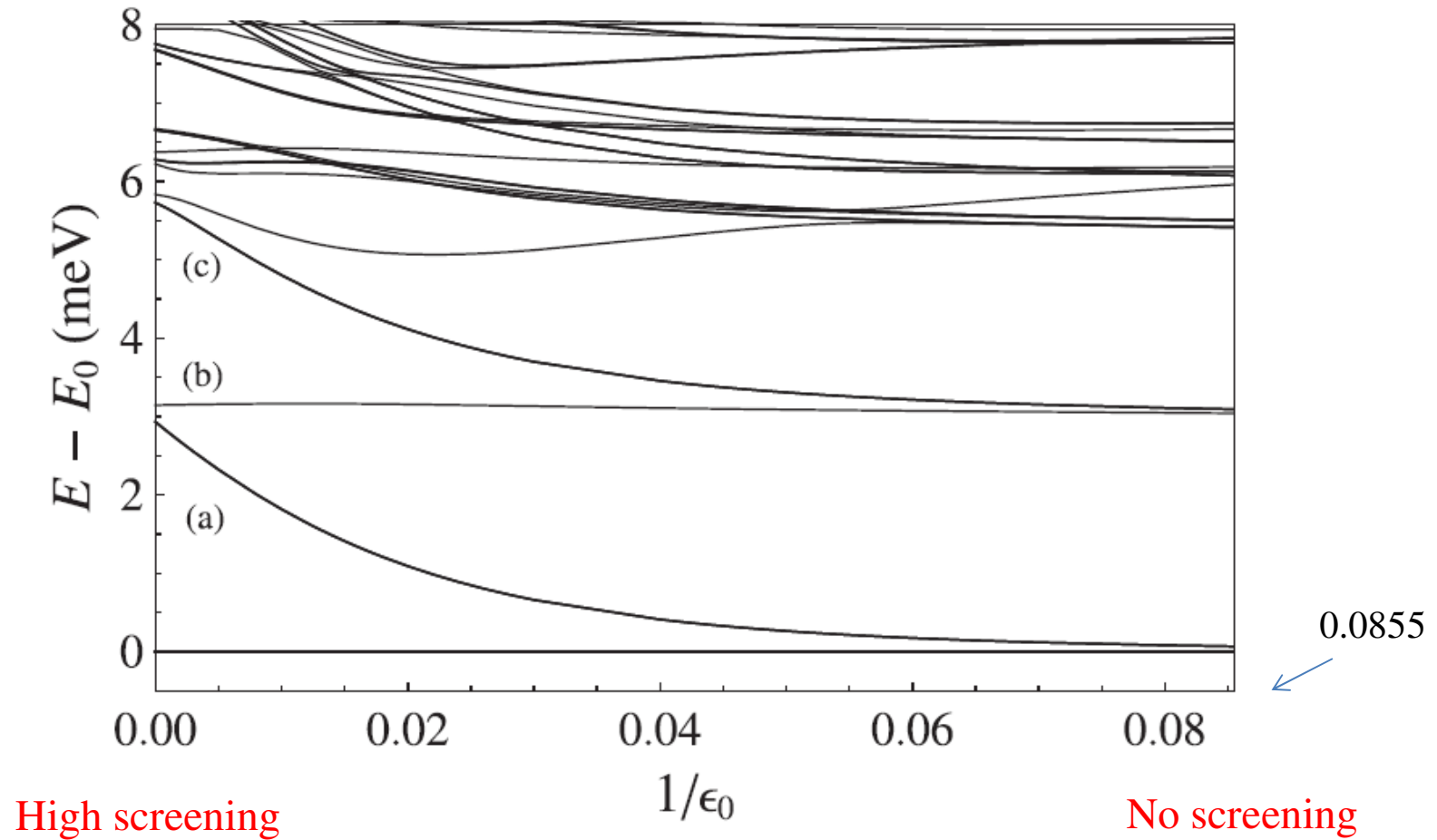
Interband (120)



Single quantum dot, two-hole excitation energies

$$V_{\text{QD}}(\mathbf{r}) = \frac{1}{2}(\kappa_x x^2 + \kappa_y y^2 + \kappa_z z^2)$$

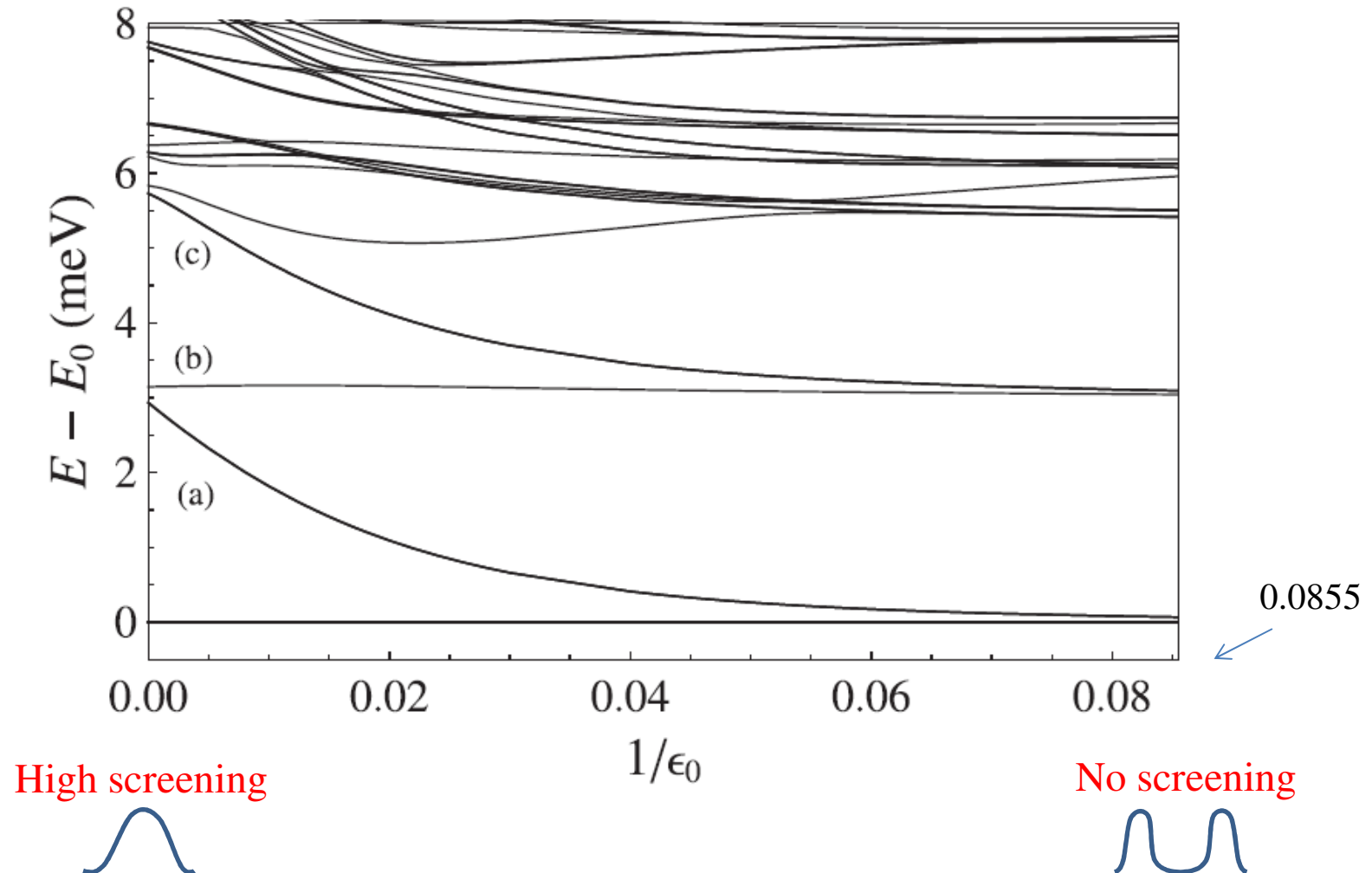
$$\ell = (10, 4, 2) \text{ nm}$$



Single quantum dot, two-hole excitation energies

$$V_{\text{QD}}(\mathbf{r}) = \frac{1}{2}(\kappa_x x^2 + \kappa_y y^2 + \kappa_z z^2)$$

$$\ell = (10, 4, 2) \text{ nm}$$



Recap (1)

- 6-band envelope-function formalism;
- Configuration-Interaction (CI) method for interacting two-hole systems;
- Intra- and inter-band Coulomb scattering processes;
- Interband Coulomb processes are relevant in a regime of high screening and/or strong confinement;
- In unscreened Si single quantum dots → two-hole Wigner molecules.

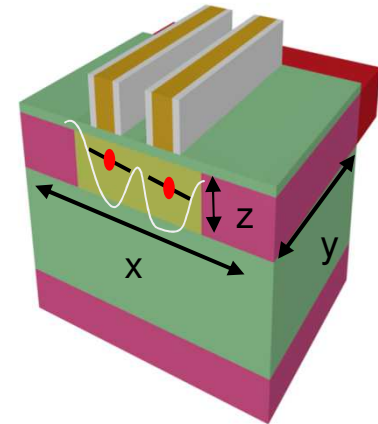
PHYSICAL REVIEW B **104**, 205409 (2021)

Inter- and intraband Coulomb interactions between holes in silicon nanostructures

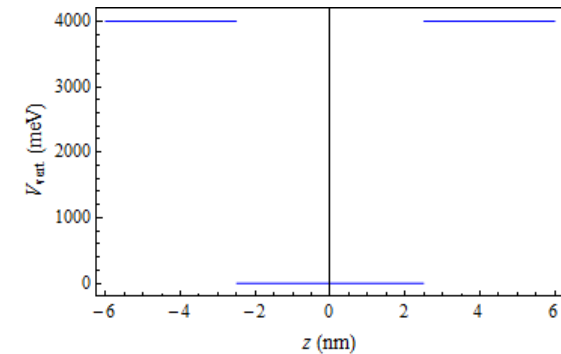
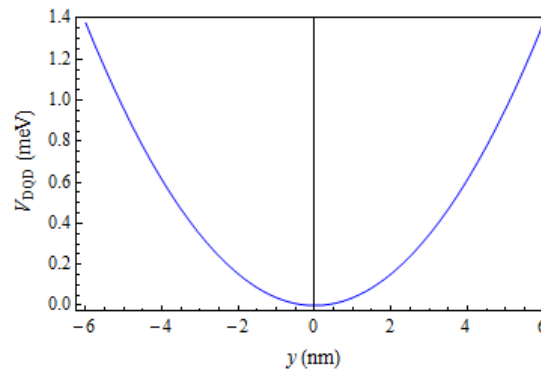
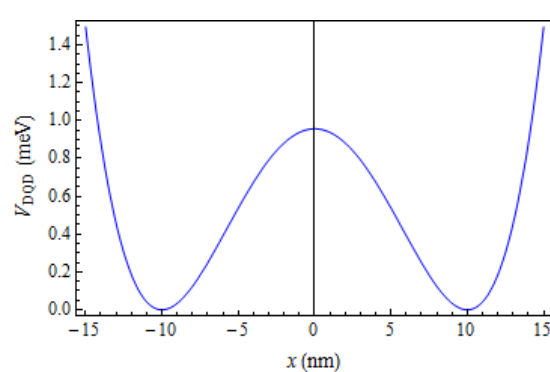
Andrea Secchi ^{*}, Laura Bellentani , Andrea Bertoni , and Filippo Troiani
Centro S3, CNR-Istituto di Nanoscienze, via G. Campi 213/A, I-41125 Modena, Italy

Double quantum dots

Two-qubit gates via exchange modulation
(Loss-Di Vincenzo proposal)



$$V(\mathbf{r}) = V_{\text{DQD}}(x) + V_{\text{QD}}(y) + V_{\parallel} \theta(|z| - L_z/2)$$



$$V_{\text{DQD}}(x) = \frac{1}{2} \kappa \frac{(x^2 - a^2)^2}{4a^2}$$

$$V_{\text{QD}}(y) = \frac{1}{2} \kappa y^2$$

$$V_{\parallel} \theta(|z| - L_z/2)$$

- approximations of realistic potentials computed with TCAD or Poisson simulations
- weak tunneling regime

A. Secchi et al., Phys. Rev. B **104**, 035302 (2021)

Single-hole states

Denoted as $|\psi_\alpha\rangle$

Because of time-reversal symmetry in the absence of a magnetic field, they are organized in Kramers doublets:

$$e_1 = e_2, \quad e_3 = e_4, \quad \dots, \quad e_{2n+1} = e_{2n+2}$$

General form:

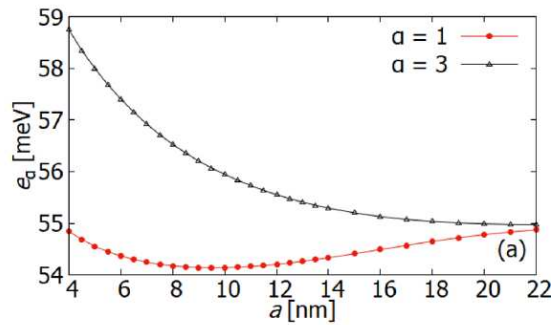
$$|\psi_\alpha\rangle = \sum_b |\psi_{\alpha,b}\rangle \otimes |b\rangle$$

band-dependent envelope function band spinor (Bloch state)
 $b = (j, m)$

This state *cannot* be factorized exactly as:

$$|\psi_\alpha^{\text{fact}}\rangle \equiv |\psi_{\alpha,1}\rangle \otimes \sum_b c_{\alpha,b} |b\rangle$$

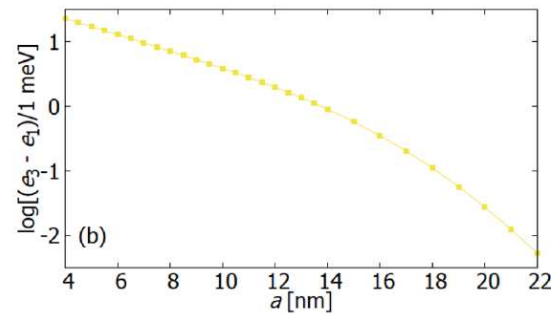
«Spin»-orbital **correlation**: the population is distributed among **different bands** and the envelope functions corresponding to different bands are **not parallel**



Si

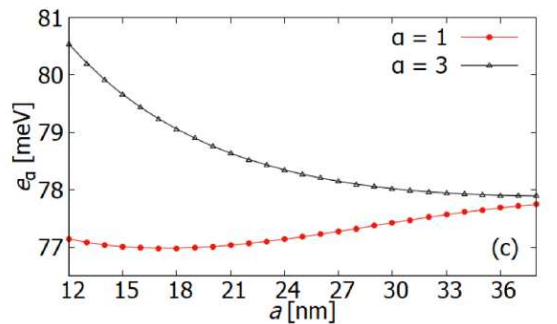
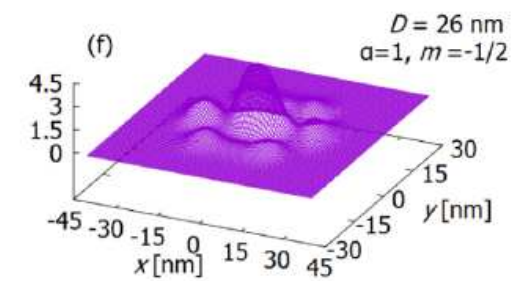
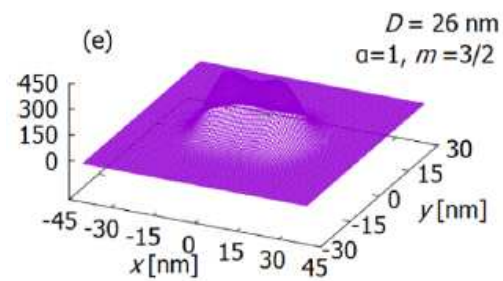
Si requires shorter interdot distances than Ge
(larger effective masses)

→ it is relevant to study the impact of **strain**

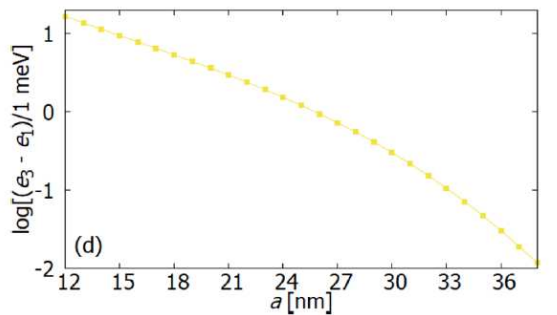
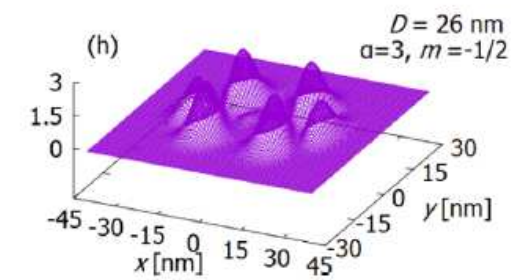
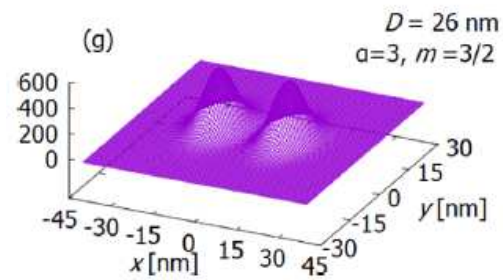


Si

Si



Ge




Ge

Dot 1

Dot 2

Band compositions and mirror symmetry

Si	$ \psi_1\rangle$		$ \psi_3\rangle$	
a (nm)	4	22	4	22
$P_{\alpha,3/2,3/2}$	0.989	0.904	0.895	0.919
$P_{\alpha,3/2,-1/2}$	0.006	0.0801	0.083	0.0643
$\langle\sigma_{yz}\rangle_{\alpha}$	0.996	1.00	-0.973	-1.00



$$\langle x, y, z | \sigma_{yz} | \psi_{\alpha} \rangle = \psi_{\alpha}(-x, y, z)$$

$$\langle \sigma_{yz} \rangle_{\alpha} = \sum_b \int dr \psi_{\alpha,b}^*(x, y, z) \psi_{\alpha,b}(-x, y, z)$$

- The **heavy-hole** component is **dominant**, followed by a small light-hole component; the split-off band is negligible \rightarrow **small entanglement**
- Single-particle states are close to being eigenstates of the **mirror symmetry** operators (with even or odd parity)
- Results for Ge are analogous; the heavy-hole weight is even larger

Two-hole states


General form: combination of Slater determinants

$$|\Psi_k\rangle = \sum_{\alpha,\beta} C_{\alpha\beta}^k |\Phi_{\alpha\beta}\rangle \quad \text{where} \quad |\Phi_{\alpha\beta}\rangle = \frac{1}{\sqrt{2}} (|\psi_\alpha\rangle|\psi_\beta\rangle - |\psi_\beta\rangle|\psi_\alpha\rangle)$$


neglect split-off bands: each hole has $j = 3/2$ (heavy and light holes)

(J, M) representation (eigenstates of square modulus and third component of total angular momentum):

$$|\Psi_k\rangle = \sum_{J,M} |\psi_{k,J,M}\rangle \otimes |J, M\rangle \quad \text{where} \quad \begin{array}{l} J \in \{0, 1, 2, 3\} \\ M \in \{-J, -J+1, \dots, J\} \end{array} \quad (16 \text{ spinors})$$



2-hole orbitals



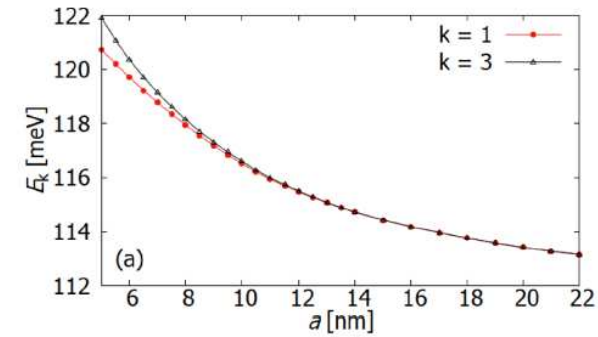
2-hole spinors

spinor weights $p_{k,J,M} = \langle \psi_{k,J,M} | \psi_{k,J,M} \rangle$

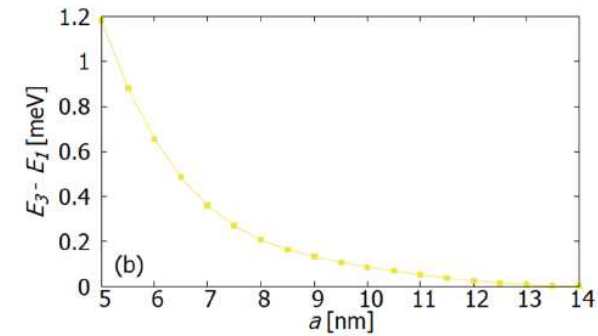
Main messages from the numerics

- Lowest energy states: **singlet and triplet**
- Complicated **spinor** structure
- The singlet-triplet gap decreases with a **faster than the single-particle gap**
- The singlet-triplet gap is significantly **larger for Ge** at the same a

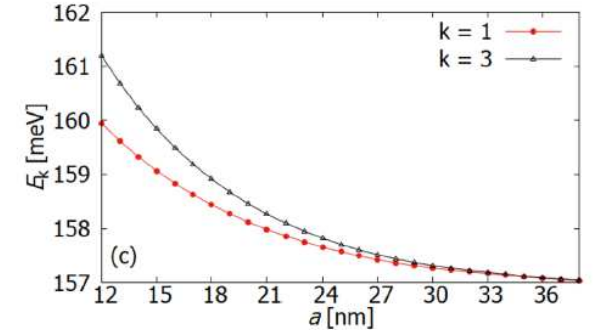
Si



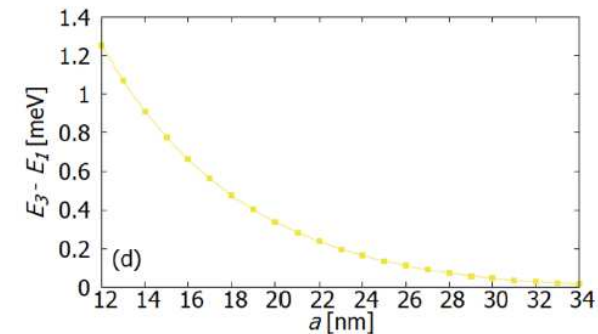
Si



Ge



Ge



Spinor compositions

(relevant for external field coupling and decoherence)

	$S (k = 1)$		$T_0 (k = 3)$		
Si	5	14	5	14	
a (nm)					
$p_{k,0,0}$	0.490	0.487	0.000	0.000	minority-symmetry terms (anti-symmetric spinors)
$p_{k,2,0}$	0.477	0.488	0.000	0.006	
$p_{k,2,\pm 2}$	0.012	0.001	0.008	0.012	
$p_{k,1,0}$	0.000	0.000	0.860	0.878	
$p_{k,3,0}$	0.000	0.000	0.099	0.098	
$p_{k,3,\pm 2}$	0.004	0.005	0.012	0.005	
Ge	$S (k = 1)$		$T_0 (k = 3)$		
a (nm)	12	34	12	34	
$p_{k,0,0}$	0.499	0.499	0.000	0.000	minority-symmetry terms (symmetric spinors)
$p_{k,2,0}$	0.499	0.499	0.000	0.000	
$p_{k,2,\pm 2}$	0.000	0.000	0.000	0.000	
$p_{k,1,0}$	0.000	0.000	0.897	0.898	
$p_{k,3,0}$	0.000	0.000	0.100	0.100	
$p_{k,3,\pm 2}$	0.000	0.000	0.000	0.000	

Effective 4-band Hubbard model

Motivation: better understanding of physics + possible extension to large arrays of qubits

$$\hat{H}_{\text{DQD}} = \hat{H}_{k \cdot p} + \underbrace{\hat{V}_1 + \hat{V}_2 + \hat{V}_{12}}_{\hat{V}_{\text{DQD}}}$$

Localized single-dot single-particle states:

$$(\hat{H}_{k \cdot p} + \hat{V}_s) |\psi_{s,\tau}\rangle = E_{s,\tau} |\psi_{s,\tau}\rangle$$

s = site index

τ = Kramers spin

Numerical calculations on the single-dots suggest the following approximation:

$$\begin{aligned} |\psi_{s,\uparrow}\rangle &\equiv |\psi_{s,H}\rangle \otimes \left(\left| \frac{3}{2} \right\rangle + \left| -\frac{3}{2} \right\rangle \right) + |\psi_{s,L}\rangle \otimes \left(\left| \frac{1}{2} \right\rangle + \left| -\frac{1}{2} \right\rangle \right) \\ |\psi_{s,\downarrow}\rangle &\equiv |\psi_{s,H}^*\rangle \otimes \left(\left| \frac{3}{2} \right\rangle - \left| -\frac{3}{2} \right\rangle \right) - |\psi_{s,L}^*\rangle \otimes \left(\left| \frac{1}{2} \right\rangle - \left| -\frac{1}{2} \right\rangle \right) \end{aligned}$$

We derive the effective model Hamiltonian

$$\begin{aligned} \hat{H}_{\text{Hubbard}} &= [T(\hat{\psi}_{1,\uparrow}^\dagger \hat{\psi}_{2,\uparrow} + \hat{\psi}_{2,\downarrow}^\dagger \hat{\psi}_{1,\downarrow}) + \text{H.c.}] \\ &\quad + U(\hat{n}_{1,\uparrow} \hat{n}_{1,\downarrow} + \hat{n}_{2,\uparrow} \hat{n}_{2,\downarrow}), \end{aligned}$$

and we solve it for $N = 1$ and 2 , comparing the solutions with the numerical results.

Solution for $N = 1$

Eigenenergies (both doubly degenerate): $e_{\pm} = \pm|T|$

NB: $T = |T|e^{i\theta}$

Eigenstates: $|\psi_{\pm,\tau}\rangle = \frac{1}{\sqrt{2}}(\hat{\psi}_{1,\tau}^{\dagger} \pm e^{-i\theta}\hat{\psi}_{2,\tau}^{\dagger})|0\rangle$

Expansion on the m basis:

$$|\psi_{\pm,\uparrow}\rangle = \frac{1}{\sqrt{2}} \left[(|\psi_{1,H}\rangle \pm e^{-i\theta}|\psi_{2,H}\rangle) \otimes \left(\left| \frac{3}{2} \right\rangle + \left| -\frac{3}{2} \right\rangle \right) \right. \\ \left. + (|\psi_{1,L}\rangle \pm e^{-i\theta}|\psi_{2,L}\rangle) \otimes \left(\left| \frac{1}{2} \right\rangle + \left| -\frac{1}{2} \right\rangle \right) \right],$$

$$|\psi_{\pm,\downarrow}\rangle = \frac{1}{\sqrt{2}} \left[(|\psi_{1,H}^*\rangle \pm e^{-i\theta}|\psi_{2,H}^*\rangle) \otimes \left(\left| \frac{3}{2} \right\rangle - \left| -\frac{3}{2} \right\rangle \right) \right. \\ \left. - (|\psi_{1,L}^*\rangle \pm e^{-i\theta}|\psi_{2,L}^*\rangle) \otimes \left(\left| \frac{1}{2} \right\rangle - \left| -\frac{1}{2} \right\rangle \right) \right].$$

Solution for $N = 1$

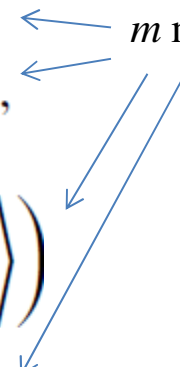
Eigenenergies (both doubly degenerate): $e_{\pm} = \pm|T|$

NB: $T = |T|e^{i\theta}$

Eigenstates: $|\psi_{\pm,\tau}\rangle = \frac{1}{\sqrt{2}}(\hat{\psi}_{1,\tau}^{\dagger} \pm e^{-i\theta}\hat{\psi}_{2,\tau}^{\dagger})|0\rangle$

Expansion on the m basis:

$$\begin{aligned}
 |\psi_{\pm,\uparrow}\rangle &= \frac{1}{\sqrt{2}} \left[(|\psi_{1,H}\rangle \pm e^{-i\theta}|\psi_{2,H}\rangle) \otimes \left(\left| \frac{3}{2} \right\rangle + \left| -\frac{3}{2} \right\rangle \right) \right. \\
 &\quad \left. + (|\psi_{1,L}\rangle \pm e^{-i\theta}|\psi_{2,L}\rangle) \otimes \left(\left| \frac{1}{2} \right\rangle + \left| -\frac{1}{2} \right\rangle \right) \right], \\
 |\psi_{\pm,\downarrow}\rangle &= \frac{1}{\sqrt{2}} \left[(|\psi_{1,H}^*\rangle \pm e^{-i\theta}|\psi_{2,H}^*\rangle) \otimes \left(\left| \frac{3}{2} \right\rangle - \left| -\frac{3}{2} \right\rangle \right) \right. \\
 &\quad \left. - (|\psi_{1,L}^*\rangle \pm e^{-i\theta}|\psi_{2,L}^*\rangle) \otimes \left(\left| \frac{1}{2} \right\rangle - \left| -\frac{1}{2} \right\rangle \right) \right].
 \end{aligned}$$

m mixing
 

Solution for $N = 1$

Eigenenergies (both doubly degenerate): $e_{\pm} = \pm|T|$

NB: $T = |T|e^{i\theta}$

Eigenstates: $|\psi_{\pm,\tau}\rangle = \frac{1}{\sqrt{2}}(\hat{\psi}_{1,\tau}^{\dagger} \pm e^{-i\theta}\hat{\psi}_{2,\tau}^{\dagger})|0\rangle$

Expansion on the m basis:

Spatial (anti)-symmetry for real T
consistent with numerical results

$$\begin{aligned}
 |\psi_{\pm,\uparrow}\rangle &= \frac{1}{\sqrt{2}} \left[(|\psi_{1,H}\rangle \pm e^{-i\theta}|\psi_{2,H}\rangle) \otimes \left(\left| \frac{3}{2} \right\rangle + \left| -\frac{3}{2} \right\rangle \right) \right. \\
 &\quad \left. + (|\psi_{1,L}\rangle \pm e^{-i\theta}|\psi_{2,L}\rangle) \otimes \left(\left| \frac{1}{2} \right\rangle + \left| -\frac{1}{2} \right\rangle \right) \right], \\
 |\psi_{\pm,\downarrow}\rangle &= \frac{1}{\sqrt{2}} \left[(|\psi_{1,H}^*\rangle \pm e^{-i\theta}|\psi_{2,H}^*\rangle) \otimes \left(\left| \frac{3}{2} \right\rangle - \left| -\frac{3}{2} \right\rangle \right) \right. \\
 &\quad \left. - (|\psi_{1,L}^*\rangle \pm e^{-i\theta}|\psi_{2,L}^*\rangle) \otimes \left(\left| \frac{1}{2} \right\rangle - \left| -\frac{1}{2} \right\rangle \right) \right].
 \end{aligned}$$

m mixing

Solution for $N = 2$

We directly consider the **Heisenberg-Hamiltonian limit** (low T/U):

$$\hat{H}_{\text{Heisenberg}} = J(\hat{\mathbf{S}}_1 \cdot \hat{\mathbf{S}}_2 - \frac{1}{4}) \quad \text{where} \quad \hat{\mathbf{S}}_s = \frac{1}{2} \sum_{\tau, \tau' \in \{\uparrow, \downarrow\}} \hat{\psi}_{s, \tau}^\dagger \boldsymbol{\sigma}_{\tau, \tau'} \hat{\psi}_{s, \tau'}$$

Eigenstates:

(**Kramers-spin operator** for site s)

$$|S\rangle \equiv \frac{1}{\sqrt{2}} (\hat{\psi}_{1, \uparrow}^\dagger \hat{\psi}_{2, \downarrow}^\dagger - \hat{\psi}_{1, \downarrow}^\dagger \hat{\psi}_{2, \uparrow}^\dagger) |0\rangle$$

Energy = $-J$

$$|T_\uparrow\rangle \equiv \hat{\psi}_{1, \uparrow}^\dagger \hat{\psi}_{2, \uparrow}^\dagger |0\rangle$$

$$|T_0\rangle \equiv \frac{1}{\sqrt{2}} (\hat{\psi}_{1, \uparrow}^\dagger \hat{\psi}_{2, \downarrow}^\dagger + \hat{\psi}_{1, \downarrow}^\dagger \hat{\psi}_{2, \uparrow}^\dagger) |0\rangle$$

$$|T_\downarrow\rangle \equiv \hat{\psi}_{1, \downarrow}^\dagger \hat{\psi}_{2, \downarrow}^\dagger |0\rangle$$

Energy = 0

Expansion of the singlet state on the (J, M) basis:

$$\begin{aligned} |\mathbb{S}\rangle = & (|\Psi_{1H,2H}^S\rangle + |\Psi_{1L,2L}^S\rangle) \otimes |0, 0\rangle \\ & + (|\Psi_{1H,2H}^S\rangle - |\Psi_{1L,2L}^S\rangle) \otimes |2, 0\rangle \\ & + \frac{1}{\sqrt{2}} (|\Psi_{1L,2H}^S\rangle + |\Psi_{1H,2L}^S\rangle) \otimes (|2, 2\rangle + |2, -2\rangle) \\ & + \frac{1}{\sqrt{2}} (|\Psi_{1L,2H}^A\rangle - |\Psi_{1H,2L}^A\rangle) \otimes (|3, 2\rangle - |3, -2\rangle) \end{aligned}$$

Expansion of the singlet state on the (J, M) basis:

$$\begin{aligned}
 |S\rangle = & (|\Psi_{1H,2H}^S\rangle + |\Psi_{1L,2L}^S\rangle) \otimes |0, 0\rangle \\
 & + (|\Psi_{1H,2H}^S\rangle - |\Psi_{1L,2L}^S\rangle) \otimes |2, 0\rangle \\
 & + \frac{1}{\sqrt{2}} (|\Psi_{1L,2H}^S\rangle + |\Psi_{1H,2L}^S\rangle) \otimes (|2, 2\rangle + |2, -2\rangle) \\
 & + \frac{1}{\sqrt{2}} (|\Psi_{1L,2H}^A\rangle - |\Psi_{1H,2L}^A\rangle) \otimes (|3, 2\rangle - |3, -2\rangle)
 \end{aligned}$$

Antisymmetric spinors

Symmetric spinors

Expansion of the singlet state on the (J, M) basis:

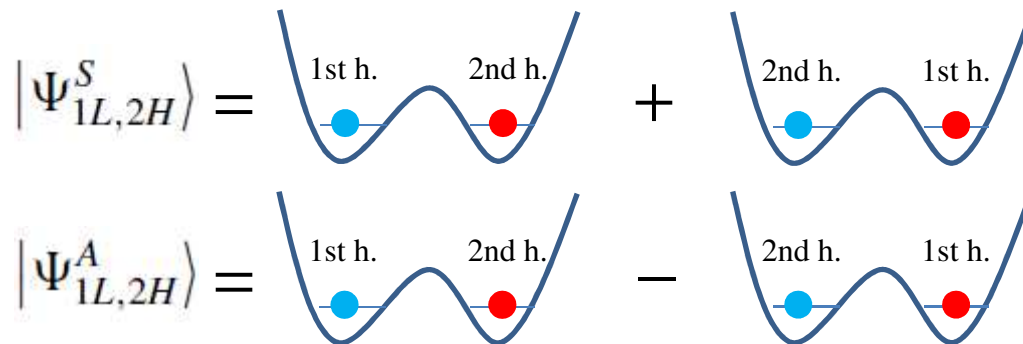
$$\begin{aligned}
 |S\rangle = & (|\Psi_{1H,2H}^S\rangle + |\Psi_{1L,2L}^S\rangle) \otimes |0, 0\rangle \\
 & + (|\Psi_{1H,2H}^S\rangle - |\Psi_{1L,2L}^S\rangle) \otimes |2, 0\rangle \\
 & + \frac{1}{\sqrt{2}} (|\Psi_{1L,2H}^S\rangle + |\Psi_{1H,2L}^S\rangle) \otimes (|2, 2\rangle + |2, -2\rangle) \\
 & + \frac{1}{\sqrt{2}} (|\Psi_{1L,2H}^A\rangle - |\Psi_{1H,2L}^A\rangle) \otimes (|3, 2\rangle - |3, -2\rangle)
 \end{aligned}$$

Symmetric orbitals

Antisymmetric spinors

Antisymmetric orbitals
(L - H mixing and non-parallelism
is necessary)

Symmetric spinors



Expansion of the singlet state on the (J, M) basis:

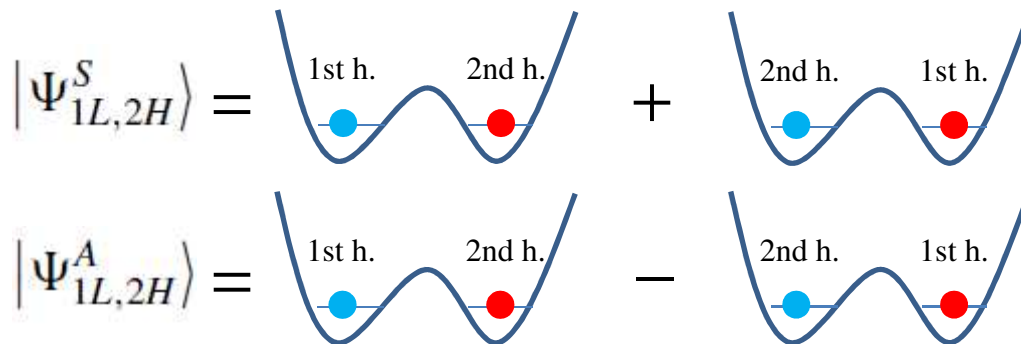
$$\begin{aligned}
 |S\rangle = & (|\Psi_{1H,2H}^S\rangle + |\Psi_{1L,2L}^S\rangle) \otimes |0, 0\rangle \\
 & + (|\Psi_{1H,2H}^S\rangle - |\Psi_{1L,2L}^S\rangle) \otimes |2, 0\rangle \\
 & + \frac{1}{\sqrt{2}} (|\Psi_{1L,2H}^S\rangle + |\Psi_{1H,2L}^S\rangle) \otimes (|2, 2\rangle + |2, -2\rangle) \\
 & + \frac{1}{\sqrt{2}} (|\Psi_{1L,2H}^A\rangle - |\Psi_{1H,2L}^A\rangle) \otimes (|3, 2\rangle - |3, -2\rangle)
 \end{aligned}$$

Antisymmetric spinors

Symmetric orbitals

Antisymmetric orbitals
(L - H mixing and non-parallelism is necessary)

Symmetric spinors



Singlet in the 2-band,
spin-1/2 case:

$$|S\rangle = |\Psi_{1,2}^S\rangle \otimes |0, 0\rangle$$

Expansion of a triplet state on the (J, M) basis:

$$\begin{aligned}
 |T_{z,+}\rangle = & \sqrt{2} |\Psi_{1H,2H}^A\rangle \otimes |3, 3\rangle \\
 & + \sqrt{2} |\Psi_{1L,2L}^A\rangle \otimes \left(\sqrt{\frac{2}{5}} |1, -1\rangle + \sqrt{\frac{3}{5}} |3, -1\rangle \right) \\
 & + (|\Psi_{1L,2H}^A\rangle + |\Psi_{1H,2L}^A\rangle) \otimes \left(\sqrt{\frac{3}{5}} |1, 1\rangle \right. \\
 & \left. - \sqrt{\frac{2}{5}} |3, 1\rangle \right) + (|\Psi_{1L,2H}^S\rangle - |\Psi_{1H,2L}^S\rangle) \otimes |2, 1\rangle,
 \end{aligned}$$

Antisymmetric orbitals \rightarrow (points to the first two terms)
 Symmetric spinors \rightarrow (points to the first two terms)
 Symmetric orbital (L - H mixing and non-parallelism is necessary) \rightarrow (points to the third term)
 Antisymmetric spinor \rightarrow (points to the fourth term)

Analogous triplet state in the 2-band, spin-1/2 case:
 $|T_{\uparrow\uparrow}\rangle = |\Psi_{1,2}^A\rangle \otimes |1, 1\rangle$

Expansion of a triplet state on the (J, M) basis:

$$\begin{aligned}
 |T_{z,+}\rangle = & \sqrt{2} |\Psi_{1H,2H}^A\rangle \otimes |3, 3\rangle \\
 & + \sqrt{2} |\Psi_{1L,2L}^A\rangle \otimes \left(\sqrt{\frac{2}{5}} |1, -1\rangle + \sqrt{\frac{3}{5}} |3, -1\rangle \right) \\
 & + (|\Psi_{1L,2H}^A\rangle + |\Psi_{1H,2L}^A\rangle) \otimes \left(\sqrt{\frac{3}{5}} |1, 1\rangle \right. \\
 & \left. - \sqrt{\frac{2}{5}} |3, 1\rangle \right) + (|\Psi_{1L,2H}^S\rangle - |\Psi_{1H,2L}^S\rangle) \otimes |2, 1\rangle,
 \end{aligned}$$

Antisymmetric orbitals \rightarrow (points to the first two terms)
 Symmetric spinors \rightarrow (points to the first term)
 Symmetric orbital (L - H mixing and non-parallelism is necessary) \rightarrow (points to the third term)
 Antisymmetric spinor \rightarrow (points to the fourth term)

Analogous triplet state in the 2-band, spin-1/2 case:
 $|T_{\uparrow\uparrow}\rangle = |\Psi_{1,2}^A\rangle \otimes |1, 1\rangle$

If we kill the L holes, we kill the minority-symmetry components and the M mixing:

$$\begin{aligned}
 |S\rangle & \rightarrow \sqrt{2} |\Psi_{1H,2H}^S\rangle \otimes \frac{1}{\sqrt{2}} (|0, 0\rangle + |2, 0\rangle), \\
 |T_{z,+}\rangle & \rightarrow \sqrt{2} |\Psi_{1H,2H}^A\rangle \otimes |3, 3\rangle, \\
 |T_{z,0}\rangle & \rightarrow \sqrt{2} |\Psi_{1H,2H}^A\rangle \otimes \frac{1}{\sqrt{10}} (3|1, 0\rangle + |3, 0\rangle), \\
 |T_{z,-}\rangle & \rightarrow \sqrt{2} |\Psi_{1H,2H}^A\rangle \otimes |3, -3\rangle.
 \end{aligned}$$

Comparison of the Hubbard model with the numerical results:

$p_{k,J,M}$ is the weight of the (J, M) spinor in state k

The model predicts specific relations between several values of $p_{k,J,M}$, **independently of the specific orbital wave functions**. For example (taken from a triplet state):

$$\dots + \sqrt{2} |\Psi_{1L,2L}^A\rangle \otimes \left(\sqrt{\frac{2}{5}} |1, -1\rangle + \sqrt{\frac{3}{5}} |3, -1\rangle \right) \dots \quad \text{implies} \quad \frac{p_{2,3,-1}}{p_{2,1,-1}} = \frac{3}{2}$$

There are 18 relations similar to this for the predicted spinor weights in the singlet and triplet.

Comparison with the numerics:


- All relations satisfied within an accuracy of $10^{-4} - 10^{-3}$
- Spinors not predicted by the model, total weight: $10^{-3} - 10^{-2}$
- Minority-symmetry states: 10^{-2}

Recap (2)

- Single- and two-hole states exhibit a small degree of entanglement, due to either small band mixing, or parallelism of the envelope functions, or both;
- They are superpositions of spinors with different eigenvalues of the angular momentum operators;
- A four-band version of the Hubbard model is able to account for the mixing (qualitatively and quantitatively);
- The source of even/odd J mixing in the two-hole states is due to the presence of distinct heavy- and light-hole envelope functions (i.e., the same source of spin-orbital entanglement);
- Possible extension to large arrays of qubits.

PHYSICAL REVIEW B **104**, 035302 (2021)

Interacting holes in Si and Ge double quantum dots: From a multiband approach to an effective-spin picture

Andrea Secchi ^{*}, Laura Bellentani, Andrea Bertoni, and Filippo Troiani
Centro S3, CNR-Istituto di Nanoscienze, I-41125 Modena, Italy

Works in progress and future works

- Study of the role of **strain** in increasing tunneling and exchange;
- Study of qubit **readout** circuits and quantum capacitance;
- Study of **decoherence** due to charge impurities and phonons.

Coworkers and IQUBITS collaborators



Laura Bellentani, Andrea Bertoni, Filippo Troiani
Bamidele I. Adetunji, Arrigo Calzolari
Elisa Molinari



Michele Spasaro
Dario Sufrà
Domenico Zito (coordinator of IQUBITS)



Matteo Bina
Andrea Padovani
Luca Larcher



Shai Bonen
Sorin P. Voinigescu

Inter- and intraband Coulomb interactions between holes in silicon nanostructures

Andrea Secchi ^{*}, Laura Bellentani , Andrea Bertoni , and Filippo Troiani
Centro S3, CNR-Istituto di Nanoscienze, via G. Campi 213/A, I-41125 Modena, Italy

Interacting holes in Si and Ge double quantum dots: From a multiband approach to an effective-spin picture

Andrea Secchi ^{*}, Laura Bellentani, Andrea Bertoni, and Filippo Troiani
Centro S3, CNR-Istituto di Nanoscienze, I-41125 Modena, Italy

Toward Hole-Spin Qubits in Si *p*-MOSFETs within a Planar CMOS Foundry Technology

L. Bellentani ¹, M. Bina,² S. Bonen ³, A. Secchi ^{1,*}, A. Bertoni,¹ S. P. Voinigescu,³ A. Padovani,²
L. Larcher,² and F. Troiani¹